JVI Journals.ASM.org

Adenovirus E1A Targets the DREF Nuclear Factor To Regulate Virus Gene Expression, DNA Replication, and Growth

Sandi Radko,[a] Maria Koleva,[a] Kris M. D. James,[b] Richard Jung,[a] Joe S. Mymryk,[b,c] Peter Pelka[a]

Department of Microbiology, University of Manitoba, Winnipeg, MB, Canada[a]; Department of Microbiology and Immunology, Western University, London, ON, Canada[b]; Department of Oncology, Western University, London, ON, Canada[c]

ABSTRACT

The adenovirus E1A gene is the first gene expressed upon viral infection. E1A remodels the cellular environment to maximize permissivity for viral replication. E1A is also the major transactivator of viral early gene expression and a coregulator of a large number of cellular genes. E1A carries out its functions predominantly by binding to cellular regulatory proteins and altering their activities. The unstructured nature of E1A enables it to bind to a large variety of cellular proteins and form new molecular complexes with novel functions. The C terminus of E1A is the least-characterized region of the protein, with few known binding partners. Here we report the identification of cellular factor DREF (ZBED1) as a novel and direct binding partner of E1A. Our studies identify a dual role for DREF in the viral life cycle. DREF contributes to activation of gene expression from all viral promoters early in infection. Unexpectedly, it also functions as a growth restriction factor for adenovirus as knockdown of DREF enhances virus growth and increases viral genome copy number late in the infection. We also identify DREF as a component of viral replication centers. E1A affects the subcellular distribution of DREF within PML bodies and enhances DREF SUMOylation. Our findings identify DREF as a novel E1A C terminus binding partner and provide evidence supporting a role for DREF in viral replication.

IMPORTANCE

This work identifies the putative transcription factor DREF as a new target of the E1A oncoproteins of human adenovirus. DREF was found to primarily localize with PML nuclear bodies in uninfected cells and to relocalize into virus replication centers during infection. DREF was also found to be SUMOylated, and this was enhanced in the presence of E1A. Knockdown of DREF reduced the levels of viral transcripts detected at 20 h, but not at 40 h, postinfection, increased overall virus yield, and enhanced viral DNA replication. DREF was also found to localize to viral promoters during infection together with E1A. These results suggest that DREF contributes to activation of viral gene expression. However, like several other PML-associated proteins, DREF also appears to function as a growth restriction factor for adenovirus infection.

The interaction of the adenovirus early 1A (E1A) proteins with mammalian regulatory factors has been heavily exploited to elucidate the molecular basis by which they control cellular processes (1–5). Studying the interactions of E1A with new cellular targets provides an exciting opportunity to identify and dissect critical mechanisms controlling mammalian transcription, growth, and differentiation, as well as to identify novel viral regulatory mechanisms. The organization of E1A into short peptide motifs (MoRFs) (6) involved in protein interactions has significantly enriched our understanding of eukaryotic protein function. Identification and characterization of novel MoRFs within E1A allow their subsequent detection in other proteins, which suggests novel interactions leading to significant changes to important pathways regulating a variety of cellular and viral processes.

Cellular regulatory proteins are organized into multinode, scale-free networks that are largely resistant to disruption (7–9). While the inherent redundancy of cellular networks prevents critical network failure upon disruption of a single node by random events (e.g., mutations), cellular networks are susceptible to targeted attacks (e.g., by pathogens) which disrupt key controllers of the network (10), namely, the "hub proteins" to which many of the subsidiary nodes connect. Where a targeted approach by a pathogen disrupts the function of the hub protein, the result is the disruption of key functions of the cellular network to which the hub protein is connected. Through the process of replication, viruses have evolved targeted and intricate molecular mechanisms by which they manipulate cellular regulatory hubs, altering the function of cellular networks in order to assist with viral proliferation (11).

Human adenoviruses (HAdVs) have unique features making them especially useful in identifying hub proteins and the cellular networks to which they are connected. HAdV normally infects noncycling cells, which are poor hosts for viral replication. Consequently, these viruses have evolved proteins that force the host cell into the cell cycle and induce expression of the cellular biosynthetic machinery and substrates that are required for efficient viral replication. The initiators and the primary executors of cell cycle modulation in HAdV-infected cells are the E1A proteins. While E1A itself does not possess an intrinsic DNA binding activity, it has been shown to alter cellular and viral gene expression on a

Received 2 September 2014 **Accepted** 4 September 2014
Published ahead of print 10 September 2014
Editor: M. J. Imperiale
Address correspondence to Peter Pelka, peter.pelka@umanitoba.ca.
M.K. and K.J. contributed equally to this work.

doi:10.1128/JVI.02538-14

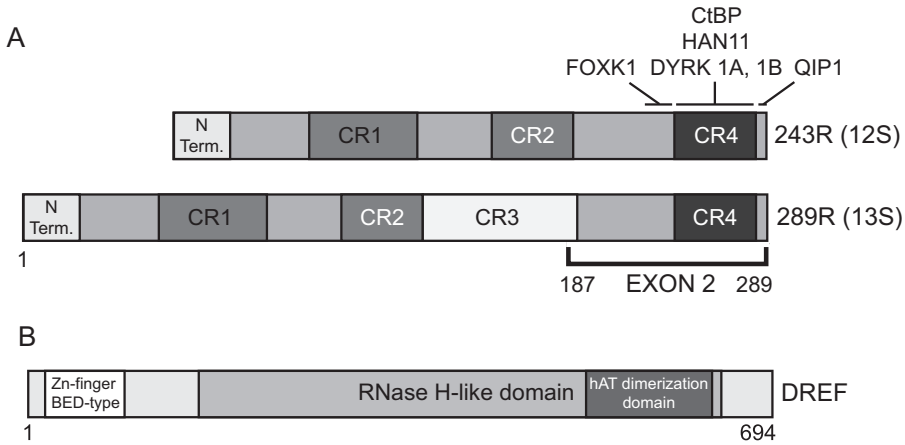

FIG 1 E1A and DREF schematic diagrams. (A) Schematic diagram of HAdV5 E1A showing the two major splice variants and conserved regions. The location of E1A exon 2 is indicated, with the residues used in MS analysis shown. (B) Schematic diagram of DREF showing key features.

large scale in order to enable viral replication (12, 13). Importantly, the most efficient way in which E1A does so is by targeting central regulatory hub proteins that control cell growth and differentiation (6). By altering the function of hub proteins in cellular networks, E1A serves as a "hub detector" by which key cellular regulators can be identified. The interaction of E1A with mammalian regulatory proteins has been heavily exploited to elucidate the molecular basis by which these hub proteins control cellular processes (1–5). Studying the interactions of E1A with recently identified binding proteins provides a unique opportunity to investigate critical mechanisms controlling mammalian transcription, growth, and differentiation.

Despite the functional importance of the C terminus of E1A and its significant contribution to the total size of E1A, very few cellular binding partners and, hence, very few MoRFs have been identified (14). The known E1A-binding partners within the region encoded by exon 2 include CtBP (15), DYRK1 (16), HAN11 (17), FOXK1/2 (17), and importin α/QIP1 (18) (Fig. 1). Each of these binds in conserved region 4 (CR4), with the exception of FOXK1. Significantly, there are E1As with C-terminal mutations (such as E267K) that bind to all the known C terminus binding partners but have impaired transformation activities, suggesting that other, as yet unidentified proteins may play a role (19).

The E1A C terminus has very few binding partners identified and remains an enigmatic part of the protein (14). To further understand the role of the C terminus of E1A during viral infection, we have used an adenovirus vector to express the C terminus of E1A (residues 187 to 289 of HAdV5 E1A) in HT1080 cells in order to isolate and identify novel proteins that specifically interact with this region of E1A. This approach identified human DREF (20) (DNA replication-related element binding factor; also known as ZBED1 [zinc finger BED-type containing]). Here we show that E1A interacts with DREF, which requires residues L272/L273 of E1A. Furthermore, during infection E1A enhances the SUMOylation of DREF and alters its subcellular distribution within nuclear PML bodies. Finally, we show that knockdown of DREF enhances viral growth, suggesting that this is a viral restriction factor. Collectively, these results demonstrate a dual role for DREF in the viral life cycle: as a coregulator of viral gene expression and a viral restriction factor.

MATERIALS AND METHODS

Antibodies. Mouse monoclonal anti-E1A M73 and M58 antibodies were previously described (21) and were grown in-house and used as the hybridoma supernatant. For immunoprecipitations (IPs), 25 μl of M73 or M58 was used, and for Western blots a dilution of 1:400 was used. Anti-hemagglutinin (anti-HA) mouse monoclonal antibody 12CA5 was previously described (22), and 25 μl of hybridoma supernatant was used in chromatin IP (ChIP) experiments. Mouse monoclonal anti-myc 9E10 antibody was previously described (23) and was grown in-house. For IPs, 50 μl of 9E10 hybridoma supernatant was used, while for Western blots the supernatant was used at 1:100 dilution. Mouse monoclonal anti-72k DNA binding protein (DBP) antibody was previously described (24) and was used at a dilution of 1:400 for Western blots. Green fluorescent protein (GFP) antibody was purchased from Clontech (catalog no. 632592) and was used at 1:4,000 dilution for Western blots; 5 μl was used for IPs. Anti-adenovirus type 5 (ab6982), anti-DREF (ab48355), anti-PML (ab53773), and anti-SUMO-1 (ab32058) antibodies were purchased from Abcam and were used at the recommended dilutions. High-affinity anti-HA rat monoclonal antibody (3F10) was purchased from Roche and was used at the recommended dilution.

Cell and virus culture. HT1080 cells (ATCC CCL-121) were grown in Dulbecco's modified Eagle's medium (HyClone) supplemented with 10% fetal bovine serum (Invitrogen), streptomycin, and penicillin (HyClone). HT1080 cells were chosen because the original mass spectrometry was carried out on HT1080 lysates and these cells do not express any viral proteins. All transfections were carried out using TurboFect reagent (Thermo-Fisher) according to the manufacturer's instructions using 10 μg of total DNA. Virus infections were carried out in serum-free media for 1 h, after which complete medium was added without removal of the infection media. All viruses used were grown in-house. Ad-LacZ was a generous gift from Frank Graham.

ChIP. ChIP was carried out essentially as previously described (1). HT1080 cells were infected with adenoviruses at a multiplicity of infection (MOI) of 10 and harvested 16 h after infection for ChIP analysis. For immunoprecipitation of E1A, the monoclonal M73 and M58 antibodies were used. For immunoprecipitation of DREF, the polyclonal anti-DREF antibody (Abcam no. ab48355) was used. Mouse monoclonal 12CA5 anti-HA antibody was used as a negative IgG control. All primers used are listed below.

PCRs were carried out for HAdV5 early and major late promoters using SYBR select master mix for CFX (Applied Biosystems) according to the manufacturer's directions, with 3% of total ChIP DNA as the template

and a CFX96 real-time PCR instrument (Bio-Rad). The annealing temperature used was 60°C, and 40 cycles were run.

Construction of Ad-X2. Ad-X2 was constructed by subcloning the HAdV5 exon 2 region from pEGFP-X2 into pCAN-Myc with the N-terminal myc tag in frame with exon 2. The myc-tagged exon 2 was subsequently subcloned using blunt-ended ligation into pAd-LoxP-WRE-SV40 (a generous gift from Arnie Berk) to generate pAd-LoxP-myc-X2. This vector was then cotransfected together with Ψ5 viral DNA into 293CRE cells to generate Ad-X2 via CRE-lox-mediated recombination as previously described (25). Following complete cytopathic effect (CPE) of transfected cells, the crude virus was tested for myc-exon 2 expression by Western blotting and subsequently plaque purified and expanded.

Immunofluorescence. HT1080 cells were plated at low density (~40,000 cells per chamber) on chamber slides (Nalgene Nunc) and subsequently infected or transfected as described above. Twenty-four hours after final transfection or infection, cells were fixed in 4% formaldehyde, blocked in blocking buffer (1% normal goat serum, 1% bovine serum albumin [BSA], 0.2% Tween 20 in phosphate-buffered saline [PBS]) and stained with specific primary antibodies. M73 was used neat (hybridoma supernatant), 3F10 rat anti-HA antibody (Roche) was used at a dilution of 1:400, PML antibody (Abcam ab53773) was used at a dilution of 1:150, 72k DBP antibody was used neat (hybridoma supernatant), DREF antibody (Abcam ab48355) was used at a dilution of 1:100, 9E10 anti-myc antibody was used neat, and Alexa Fluor 488- and 594-conjugated secondary antibodies (Jackson ImmunoResearch) were used at a dilution of 1:600. After staining and extensive washing, slides were mounted using Prolong Gold with DAPI (4′,6-diamidino-2-phenylindole; Invitrogen) and imaged using a Zeiss LSM700 confocal laser scanning microscope. Images were analyzed using the Zeiss ZEN software package.

Immunoprecipitation. Transfected HT1080 cells were lysed in NP-40 lysis buffer (0.5% NP-40, 50 mM Tris [pH 7.8], 150 mM NaCl) supplemented with a protease inhibitor cocktail (Sigma). One milligram of the cell lysate was used for IP with the monoclonal M73 anti-E1A antibody or monoclonal 9E10 anti-myc antibody. E1A was detected using the M73 monoclonal antibody, while DREF and SUMO were detected using the anti-HA rat monoclonal antibody (clone 3F10; Roche).

Mass spectrometry. Mass spectrometry sample preparation was carried out as described for "Immunoprecipitation," with a few modifications as outlined below. 9E10 and M73 antibodies were cross-linked to protein A-Sepharose beads using dimethyl pimelimidate as previously described (26). For affinity purification, 20 15-cm plates of 90% confluent HT1080 cells were infected with Ad-X2 expressing the myc-tagged C terminus of E1A at an MOI of 100 and harvested 24 h later. Five washes of 50 volumes of immunoprecipitation buffer were carried out prior to elution. Elution was carried out using 0.2 M glycine, pH 2. Samples were concentrated using Vivaspin columns (Millipore) and dialyzed against PBS. Associated proteins were resolved by SDS-PAGE and stained with Colloidal Blue. Bands present in Ad-X2-infected cells but absent in uninfected-control IPs were excised from the gel and sent to Genome Québec at McGill University for liquid chromatography-tandem mass spectrometry (LC-MS/MS)-based protein identification.

PCR primers. The following is a list of all primers used in quantitative PCR (qPCR) assays (F, forward primer; R, reverse primer; p, promoter primer used for ChIP): E4p-2-R (GGCTTTCGTTTCTGGGCGTA), E4p-2-F (TAAACACCTGAAAAACCCTCCTGCC), E3p-R (CGCCCTCTGATTTTCAGGTG), E3p-F (CGCGGGACCCCACATGATAT), E2p-R (AGAATTCGGTTTCGGTGGGC), E2p-F (AGCAAATACTGCGCGCTGAC), MLate-p-R (AACTTTATGCCTCGCGCGGG), MLate-p-F (TCGGCCTCCGAACGGTAAGA), E2A-R (GCGGATGAGGCGGCGTATCGAG), E2A-F (GGGGGTGGTTTCGCGCTGCTCC), E4orf6/7-R (TCCACCTTGCGGTTGCTTAA), E4orf6/7-F (CTGCTGCCCGAATGTAACACT), E3A-R (CTCGGAGAGGTTCTCTCGTAGACT), E3A-F (GCCGCCACAAGTGCTTTG), E1B-R (TCAAACGAGTTGGTGCTCATG), E1B-F (CGCGCTGAGTTTGGCTCTAG), Hexon-R (GGAGTACATGCGGTCCTTGT), Hexon-F (CTTACCCCCAACGAGTTTGA), E1A-R (GCTCAGGTTCAGACACAGGACTGTA), E1A-F (CACGGTTGCAGGTCTTGTCATTAT), hGAPDH-R (TTGATTTTGGAGGGATCTCG), hGAPDH-F (GAGTCAACGGATTTGGTCGT).

Plasmids. The expression plasmid for HA-DREF was previously described (20); pcDNA3.1-E1A was previously described (27), and it expresses all E1A isoforms. Plasmids for expression of E1A243R, E1A289R, GFP fusions of E1A fragments, and GFP fusions of representative E1As from different HAdV serotypes were all previously described (2). pcDNA3-HA-SUMO plasmids, generously gifted by Ron Hay, express SUMO isoforms N-terminally tagged with HA and were previously described (28). pCAN-myc-DREF was made by subcloning DREF in frame with the N-terminal myc tag.

Protein purification and GST pulldown assay. Glutathione *S*-transferase (GST) fusions of DREF fragments were made by subcloning the cDNA into pGEX-6P1 (GE Healthcare Life Sciences) in frame with the N-terminal GST tag. His-tagged E1A289R was made by subcloning the entire E1A289R cDNA into the pET42 vector (Novagen) in frame with a C-terminal 6×His tag. Proteins were expressed in *Escherichia coli* and purified on their respective resins according to the manufacturer's specifications. GST pulldowns were carried out as previously described (1).

Real-time gene expression analysis. HT1080 cells were infected with *dl*309 at an MOI of 5, and 16, 20, and 48 h after infections total cellular RNA was extracted using the TRIzol reagent (Sigma) according to the manufacturer's instructions. Total RNA (1.25 μg) was used in reverse transcriptase reactions using SuperScript VILO reverse transcriptase (Invitrogen) according to the manufacturer's guidelines and random hexanucleotides for priming. The cDNA was subsequently used for real-time expression analysis using the Bio-Rad CFX96 real-time thermocycler. Fold changes in expression were determined by comparing expression levels with levels for control knockdown cells and analyzing expression data using the Pfaffl method (29). All primers used are listed above.

siRNA knockdown. Small interfering RNA (siRNA) knockdown was carried out as previously described (1). Briefly, HT1080 cells were transfected with DREF-specific Silencer Select siRNA (Life Technologies no. s17567) using SilentFect reagent (Bio-Rad) according to the manufacturer's specifications and a 5 nM final siRNA concentration. Silencer Select negative-control siRNA no. 1 (Life Technologies) was used as the negative siRNA control.

Viral genome quantification. Infected HT1080 cells (6.0×10^5) were lysed in lysis buffer (50 mM Tris [pH 8.1], 10 mM EDTA, and 1% SDS) on ice for 10 min. Lysates were sonicated briefly in a Covaris M220 focused ultrasonicator to break up cellular chromatin and subjected to digestion using proteinase K (New England BioLabs) according to the manufacturer's specifications. Following proteinase K digestion, viral DNA was purified using a GeneJET PCR purification kit (Thermo-Fisher). PCRs were carried out using SYBR select master mix for CFX (Applied Biosystems) according to the manufacturer's directions with 2% of total purified DNA as the template and a CFX96 real-time PCR instrument (Bio-Rad). A standard curve for absolute quantification was generated by serially diluting the pXC1 plasmid containing the left end of the HAdV5 genome from a starting concentration of 1.0×10^7 copies per reaction down to 1.0 copy per reaction. The primers used were the same as those used for expression analysis of the E1B region; the annealing temperature used was 60°C, and 40 cycles were run.

Virus growth assay. HT1080 cells were infected with HAdV5 *dl*309 at an MOI of 1. Virus was adsorbed for 1 h at 37°C under 5% CO_2, after which the media were removed and cells were washed 5 times with PBS. Cells were bathed in new media and were reincubated at 37°C under 5% CO_2. Virus titers were determined 24, 48, and 72 h after infection, and plaque assays were performed on 293 cells by serial dilution.

RESULTS

DREF is a novel E1A-binding protein. Compared to the other regions of E1A, comparatively fewer binding partners have been

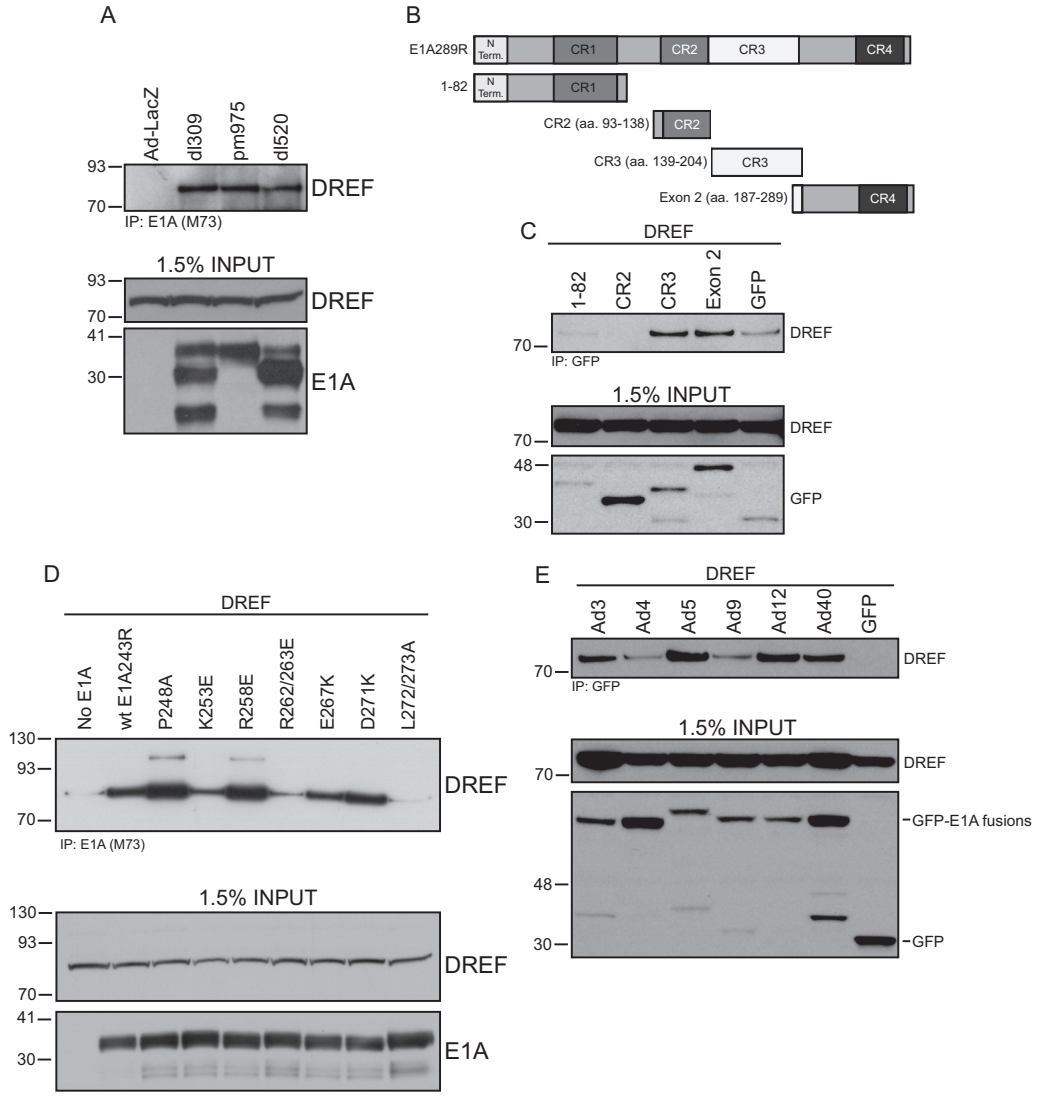

FIG 2 E1A interacts with DREF. (A) Subconfluent human HT1080 fibrosarcoma cells were infected with HAdV5 *dl*309, *pm*975, or *dl*520 expressing genomic E1A, E1A289R, or E1A243R, respectively, or Ad-LacZ with the E1 region deleted, for 24 h. Cells were subsequently harvested, lysed, and subjected to IP using M73 monoclonal anti-E1A antibody. IPs were resolved on 4 to 12% gradient Novex Bolt gels, and DREF was detected using rabbit polyclonal anti-DREF antibody. Part of the cell lysate used in the IPs (1.5%) was used as the input control. (B) Schematic representation of E1A289R and fragments fused to GFP. (C) Human HA-tagged DREF was cotransfected together with plasmids expressing the indicated GFP-E1A fragment fusions or GFP alone as a control into HT1080 human fibrosarcoma cells. Twenty-four hours after transfections cells were harvested and immunoprecipitated for GFP. IPs were resolved on 4 to 12% gradient Novex Bolt gels, and DREF was detected with anti-HA (3F10) monoclonal antibody. The input control was 1.5% of the cell lysate used in the IPs. (D) Human HA-tagged DREF was cotransfected together with plasmids expressing the indicated E1A243R single-amino-acid-substitution mutants into HT1080 human fibrosarcoma cells. An empty plasmid (pcDNA3) was used in the "no E1A" control transfection. Twenty-four hours after transfections cells were harvested and immunoprecipitated for E1A (M73). IPs were resolved on 4 to 12% gradient Novex Bolt gels, and DREF was detected with anti-HA (3F10) monoclonal antibody. The input control was 1.5% of the cell lysate used in the IPs. (E) Human HA-tagged DREF was cotransfected together with plasmids expressing indicated GFP-E1A fusions from various HAdV species into HT1080 human fibrosarcoma cells. GFP plasmid was used as a control. Twenty-four hours after transfections cells were harvested and immunoprecipitated for GFP. IPs were resolved on 4 to 12% gradient Novex Bolt gels, and DREF was detected with anti-HA (3F10) monoclonal antibody. The input control was 1.5% of the cell lysate used in the IPs.

identified for the C terminus of E1A (14). In addition to importin α, CtBP, DYRK1, HAN11, and FOXK1/2 have been identified as bona fide C terminus binding proteins (14). In order to better understand the functional contribution of E1A to the overall role of the protein during viral infection, we undertook a mass spectrometry (MS)-based identification of proteins that interact with the C terminus of HAdV5 E1A. We constructed an adenovirus vector that expresses a myc-tagged version of E1A residues 187 to 289 under the control of a cytomegalovirus (CMV) promoter. This virus was used to infect HT1080 cells and a combination of M73 anti-E1A and 9E10 anti-myc antibodies was used to affinity purify C terminus-associated proteins from cell lysates. One of the proteins identified via this approach was human DREF. To verify that E1A interacts with DREF, we carried out a coimmunoprecipitation (co-IP) in HAdV-infected HT1080 cells (Fig. 2). Endogenous DREF was found to interact with E1A in infected HT1080

cells, binding to both E1A243R and E1A289R (Fig. 2A). Using a panel of E1A fragments fused to GFP (Fig. 2B), we were able to map the interaction to two sites on E1A, CR3 and the region encoded by exon 2 (Fig. 2C).

DREF interacted with wild-type (wt) E1A243R (Fig. 2A), and since this E1A isoform lacks CR3 (Fig. 1A), the interaction with the C terminus is sufficient for stable binding. In order to further refine the region required for the interaction between the E1A C terminus and DREF, we carried out co-IPs with previously described E1A243R point mutants within E1A CR4 (19). DREF interacted, to various degrees, with all point mutants except a double mutant with leucine residues 272 and 273 mutated to alanines (Fig. 2D). Mutants that interacted most strongly with DREF also brought down a high-molecular-weight isoform of DREF (Fig. 2D, mutants P248A and R258E) that migrated slightly above the 93-kDa molecular mass marker. In order to determine whether DREF is a common target of all HAdV serotypes, we performed co-IP with GFP fusions of representative E1As from 6 different HAdV species (from species A to F) (Fig. 2E). DREF was found to interact, to various degrees, with all the different E1As suggesting that it is a universal target of human adenovirus.

Although there are only a few known C terminus binding proteins, there is a possibility that DREF interacts with E1A via an intermediary factor. Indeed, the same point mutant that appears to lose binding to DREF (E1A243R L272/273A) showed a loss of binding to DYRK1A and reduced binding to HAN11 (19). To determine whether the interaction between DREF and E1A is direct, we employed a GST pulldown assay with bacterially expressed and purified DREF fragments and bacterially expressed and purified His-tagged HAdV5 E1A289. E1A was found to interact directly with residues 315 to 694 of DREF in the GST pulldown assay (Fig. 3).

Together, these results show, for the first time, that DREF is a novel E1A-binding protein that interacts directly with E1A.

E1A likely binds to DREF via a novel MoRF and alters DREF SUMOylation. Sequence alignment of the region in CR4 of E1A where DREF binds shows a high degree of conservation between the different HAdV serotypes (Fig. 4A). Importantly, the two leucine residues necessary for the interaction of HAdV5 E1A with DREF are 100% conserved across all HAdV serotypes analyzed. To determine whether this region constitutes a novel MoRF, we took the sequence surrounding L272/273 of HAdV5 and subjected it to protein BLAST. Several human cellular proteins with similar sequences were identified, with the ubiquitin-specific peptidase-like protein 1 (USPL1) having the highest degree of similarity (Fig. 4A). USPL1 is a SUMO-specific isopeptidase that is responsible for SUMO removal from modified proteins. USPL1 is also targeted to Cajal bodies and plays a role in snRNA transcription by RNA polymerase II (30). Based on these results, we hypothesized that DREF is SUMOylated and that the interaction with E1A could affect this modification. To test this, DREF was cotransfected with HA-tagged SUMO-1, -2, or -3. DREF was immunoprecipitated and blotted for the presence of SUMO. DREF was found to be SUMOylated by SUMO-1 specifically, and expression of E1A enhanced the degree of DREF SUMOylation (Fig. 4B).

E1A was previously reported to interact with UBC9, a SUMO conjugase (31, 32). Interaction of E1A with UBC9 is required for alteration of PML body morphology in E1A-expressing cells (31), and this is abolished by the loss of E1A binding to UBC9 by the E1A T123H mutant. We next determined whether different isoforms of E1A have differing effects on DREF SUMOylation and whether interaction with DREF or UBC9 was required for alteration of DREF SUMOylation by E1A. E1A243R and E1A289R, as well as expression of all E1A isoforms (E1A genomic), enhanced DREF SUMOylation (Fig. 4C and D). Furthermore, mutant E1As unable to bind DREF (L272/273A) or bind UBC9 (T123H) did not enhance DREF SUMOylation.

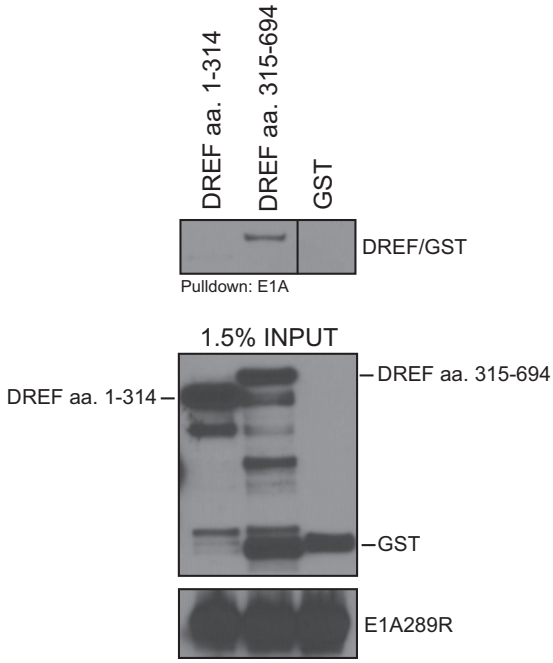

FIG 3 E1A directly interacts with DREF. Bacterially purified and GST-fused fragments of DREF were mixed with bacterially expressed and purified His-tagged E1A289R and collected using Ni-nitrilotriacetic acid resin. Pulldowns were resolved on 4 to 12% gradient Novex Bolt gels. DREF was detected using a polyclonal anti-DREF antibody, GST was detected using a polyclonal anti-GST antibody, and input E1A was detected using the M73 antibody.

Finally, to determine whether SUMOylation of endogenous DREF is altered in the context of a productive viral infection, HT1080 cells were infected with either Ad-LacZ, which does not express E1A and should not replicate, or *dl*309, which expresses wt genomic E1A (Fig. 4D). In this context, we observed enhanced SUMOylation of DREF only when E1A was present.

Together, these results identify a potential novel MoRF in E1A that is present in other cellular proteins, specifically USPL1. Furthermore, we show, for the first time, that E1A enhances the SUMOylation state of a cellular protein, DREF, during viral infection and that mutants of E1A that are unable to bind the SUMO conjugase UBC9 or DREF are deficient for this activity.

Interaction with E1A alters the subcellular distribution of DREF. E1A is known to alter the subcellular distribution of proteins in order to alter their function (27), and we have previously observed altered PML body morphology upon expression of E1A in human cells (33) that was dependent on the ability of E1A to bind to UBC9 (31). Therefore, we next investigated the subcellular localization of DREF and whether E1A alters this distribution. DREF was found to localize to the nuclei of HT1080 cells in distinct spots (Fig. 5A). Upon expression of E1A by transfection, DREF continued to localize in a punctate pattern. However, the nuclear foci appeared larger and more numerous (Fig. 5A). As

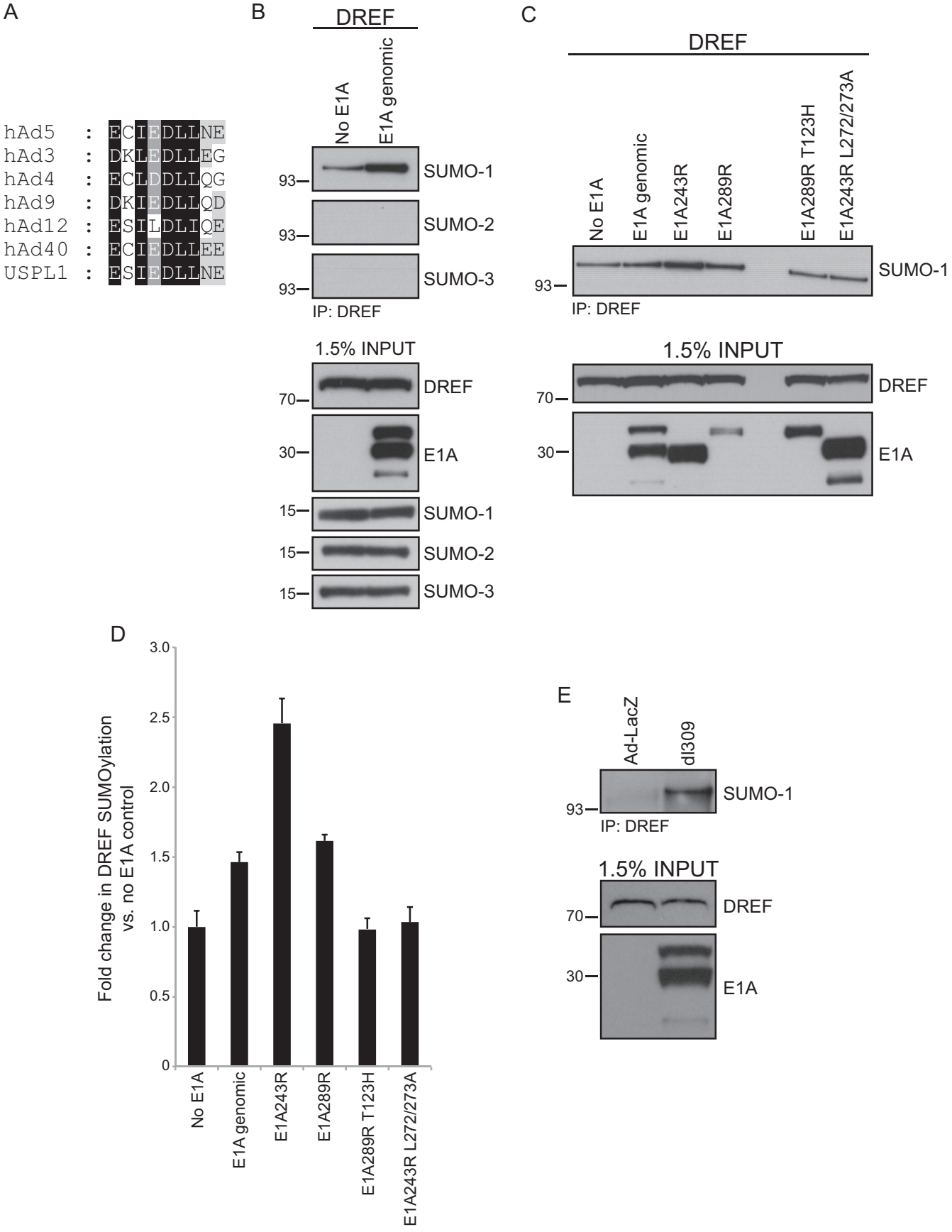
A
hAd5 : ECIEDLLNE
hAd3 : DKLEDLLEG
hAd4 : ECLDDLLQG
hAd9 : DKIEDLLQD
hAd12 : ESILDLIQE
hAd40 : ECIEDLLEE
USPL1 : ESIEDLLNE
B
DREF
No E1A
E1A genomic
93
SUMO-1
93
SUMO-2
93
SUMO-3
IP: DREF
1.5% INPUT
70
DREF
30
E1A
15
SUMO-1
15
SUMO-2
15
SUMO-3
C
DREF
No E1A
E1A genomic
E1A243R
E1A289R
E1A289R T123H
E1A243R L272/273A
93
SUMO-1
IP: DREF
1.5% INPUT
70
DREF
30
E1A
D
Fold change in DREF SUMOylation vs. no E1A control
3.0
2.5
2.0
1.5
1.0
0.5
0
No E1A
E1A genomic
E1A243R
E1A289R
E1A289R T123H
E1A243R L272/273A
E
Ad-LacZ
dl309
93
SUMO-1
IP: DREF
1.5% INPUT
70
DREF
30
E1A

E1A was previously found to alter the number and size of PML bodies in infected cells, we suspected that DREF was colocalized with PML bodies (31, 33). Furthermore, SUMOylation is a key feature of many PML-associated proteins, and we observed altered SUMOylation of DREF (Fig. 4). We next tested whether DREF itself is a component of PML bodies. Indeed, we observed that DREF colocalized with PML nuclear bodies (Fig. 5B). Interestingly, E1A appeared to alter the distribution of DREF within PML bodies to a peripheral location with minimal signal overlap with PML itself (Fig. 5B, DREF+E1A). This redistribution was lost when E1A was no longer able to bind to DREF (Fig. 5B, DREF+E1A L272/273A) but was restored again when a mutant of E1A still able to bind to DREF was coexpressed with DREF (Fig. 5B, DREF+E1A D271K). Quantification of PML bodies with overlapping DREF staining showed that the percentage dropped from approximately 90% in non-E1A-expressing cells to less than 25% when E1A was present (Fig. 5C). Together, these results identify the subcellular localization of DREF and show that E1A appears to relocalize DREF within PML bodies.

DREF is a negative regulator of viral growth and localizes to viral replication centers. To investigate the effects of DREF on viral replication, we knocked down the expression of DREF using commercially available siRNA (Fig. 6). We observed efficient knockdown of the protein as early as 24 h after initial siRNA transfection (data not shown). Knockdown of DREF caused an ~3-fold enhancement of viral titers 72 h after infection. Virus growth was enhanced following DREF knockdown as early as 48 h after infection, when detectable titers of virus were present. Enhanced growth of virus in DREF knockdown cells persisted until 72 h after infection, when final titers were determined (Fig. 6A), at which point complete cytopathic effect was observed for control and DREF knockdown cells.

The enhanced viral titers observed upon DREF knockdown suggested that DREF might be a viral restriction factor that inhibits virus growth or assembly. We next tested whether DREF itself localizes to viral replication centers and whether these were affected by DREF knockdown. HT1080 cells were stained for DREF and the viral E2A 72k DNA binding protein (DBP) 24 h after infection (Fig. 6B, top row). As expected, in cells treated with a control siRNA, the 72k DBP localized to distinct subnuclear domains (Fig. 6B, top row), which constitute the viral replication centers reported by others (34, 35). DREF colocalized with the 72k DBP. In DREF knockdown cells, 72k DBP staining was morphologically different (Fig. 6B, middle row). The 72k DBP was not present in distinct subnuclear domains and formed a more diffuse structure around the periphery of the nuclear membrane. PML bodies were also disrupted by DREF knockdown compared to those in infected cells treated with control siRNA (Fig. 6B, compare bottom row to middle row).

Collectively, these results show that DREF is localized to viral replication centers and negatively regulates viral growth. Disruption of DREF also appears to alter the localization of the 72k DBP and presumably viral replication centers within infected cells.

Knockdown of DREF inhibits viral gene expression and enhances viral genome replication. We next investigated whether the enhanced virus titers observed upon DREF knockdown were related to changes in viral gene expression. DREF is a putative transcription factor (20, 36), and the *Drosophila* homologue of DREF regulates expression of genes involved in the cell cycle (37). Since E1A alters the expression of many cell cycle-regulated genes and viral early promoters are regulated by cell cycle-dependent transcription factors such as E2F, it was logical to investigate how DREF affects viral gene expression. DREF was knocked down using siRNA in HT1080 cells, and viral mRNA expression was assessed at 20 and 40 h after infection (Fig. 7A). Overall, viral mRNA expression was consistently reduced upon DREF knockdown 20 h after infection, with hexon affected to the greatest degree (Fig. 7A). Examination of viral protein expression also showed significantly reduced expression of E1A and 72k DBP 20 h after infection (Fig. 7B). Furthermore, viral structural proteins were also reduced at 20 h after infection; however, their levels were very low at this time point (Fig. 7B, left panel). Viral gene expression and protein levels were mostly affected earlier in the infection, as 40 h after infection there was a minimal difference in levels of gene expression, with E1A showing slightly higher expression in knockdown cells versus control (Fig. 7A) and most other genes being minimally affected. Furthermore, there was no difference in viral protein levels between the control knockdown cells and cells where DREF was depleted at 40 h after infection (Fig. 7B, right panel).

The reduced viral gene expression could be caused by several factors, including reduced viral DNA replication in cells in which DREF was knocked down using DREF-specific siRNA (siDREF). To investigate how knockdown of DREF affected viral genome copy number, we assayed for viral genomes in *dl*309-infected HT1080 cells following knockdown at 10, 20, and 40 h after infection (Fig. 7C). Unexpectedly, knockdown of DREF increased viral genome copy number, leading to nearly a 100-fold increase in genome copies per cell at 40 h after infection. There was no significant difference in genome copy number at 10 and 20 h after infection. This raised the possibility that the infection is further along in siDREF knockdown cells than in control knockdown cells. Imaging of *dl*309-infected HT1080 cells at 40 h after infection showed CPE only in siDREF-treated cells, not in cells treated with nonspecific siRNA (siControl) (Fig. 7D).

FIG 4 Identification of a new MoRF in the E1A C terminus that contributes to enhanced DREF SUMOylation. (A) Multiple-sequence alignment fragments of CR4 from HAdV E1As from different serotypes together with cellular protein USPL1 highlighting amino acid conservation. Black shading indicates conservation across all species and proteins, whereas gray shading indicates only partial conservation. (B) pCAN-Myc-DREF expressing myc-tagged DREF was cotransfected into HT1080 cells together with plasmids expressing the indicated HA-tagged SUMO and genomic E1A or a control plasmid expressing no E1A. Total DREF was immunoprecipitated using the anti-myc (9E10) monoclonal antibody. IPs were resolved on a 4 to 12% gradient Novex Bolt gel, and SUMOylated isoforms of DREF were detected using anti-HA (3F10) antibody. The input control was 1.5% of the cell lysate used in the IPs. (C) Same as panel B except that the indicated isoforms of HAdV5 E1As were used in addition to two mutants: E1A289R T123H, which does not bind UBC9, and E1A243R L272/273A, which does not bind to DREF. The input control was 1.5% of the cell lysate used in the IPs. (D) Densitometric quantification of results presented in panel C normalized to the negative control (no E1A; $n = 3$; error bars represent standard deviations of results for the biological replicates). (E) Subconfluent HT1080 cells were infected with either Ad-LacZ with the E1 region deleted or HAdV5 *dl*309 as indicated. Twenty-four hours after infection endogenous DREF was immunoprecipitated using polyclonal anti-DREF antibody and resolved on a 4 to 12% gradient Novex Bolt gel. SUMOylated DREF was subsequently detected using rabbit monoclonal anti-SUMO-1 antibody. DREF was detected using polyclonal anti-DREF antibody, and E1A was detected using monoclonal M73 anti-E1A antibody. The input control was 1.5% of the cell lysate used in the IPs.

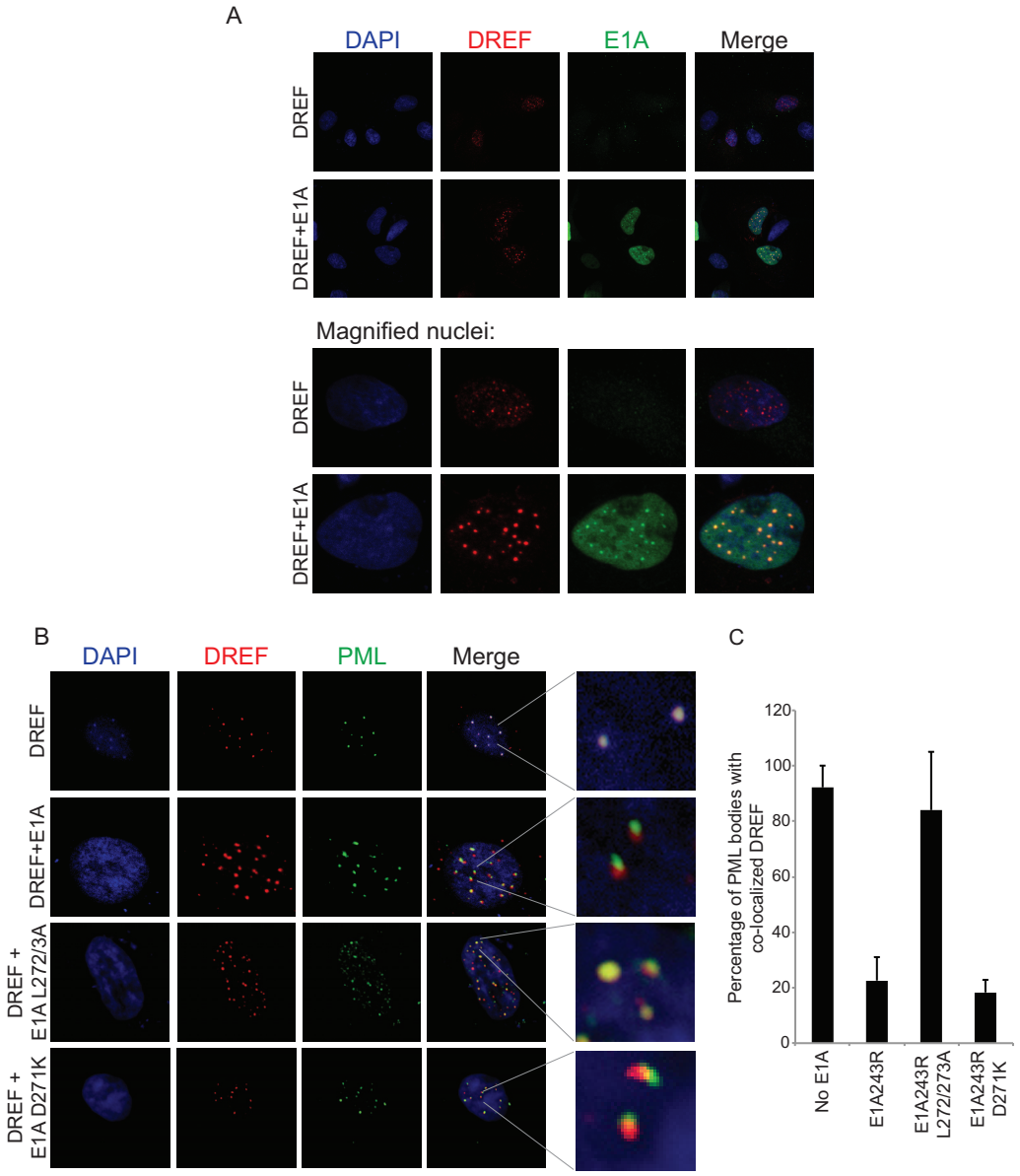

FIG 5 E1A alters the subcellular distribution of DREF. (A) HT1080 cells were transfected with a plasmid expressing HA-tagged DREF alone or together with pcDNA3.1-E1A expressing genomic HAdV5 E1A. Cells were fixed 24 h after transfection and stained for DREF using anti-HA antibody (3F10) and for E1A using anti-E1A (M73) antibody. DAPI was used as a nuclear counterstain. (B) Same as in panel A except DREF was costained with anti-PML antibody in the presence or absence of wild-type E1A243R or the indicated point mutants. (C) Quantification of the phenotype observed in panel B. Seven random nuclei from HT1080 cells cotransfected with plasmids expressing DREF and the indicated E1A243R substitution point mutants were scored for the total number of PML bodies and the number of PML bodies with overlapping DREF staining. Data are represented as percentages of PML bodies with overlapping DREF staining; error bars represent the standard deviations between results for the nuclei.

Our observation of reduced viral gene expression upon DREF knockdown 20 h after viral infection suggested that DREF might be recruited to viral promoters in order to coregulate their expression. DREF binds to specific sequences in promoters of cellular genes (20), and sequence analysis identified several potential sites in viral promoters that could be bound by DREF (data not shown). However, none of the predicted DREF-binding sites showed perfect conservation of the sequence to the predicted DREF consensus binding site (not shown). To determine whether DREF binds to viral promoters, we performed chromatin immunoprecipitation for E1A and DREF at the major late promoter (MLP) and E2, E3, and E4 promoters (Fig. 8). Both E1A and DREF were found on all promoters tested, and we observed significant enrichment over an IgG negative-control immunoprecipitation. These results implicate DREF as playing a role in directing viral early and late gene expression.

DISCUSSION

Although it has been more than 2 decades since the discovery of CtBP as one of the first E1A C terminus binding proteins (15), very few additional polypeptides have been reported to bind to this region. E1A is thought to be a cellular network disruptor (6),

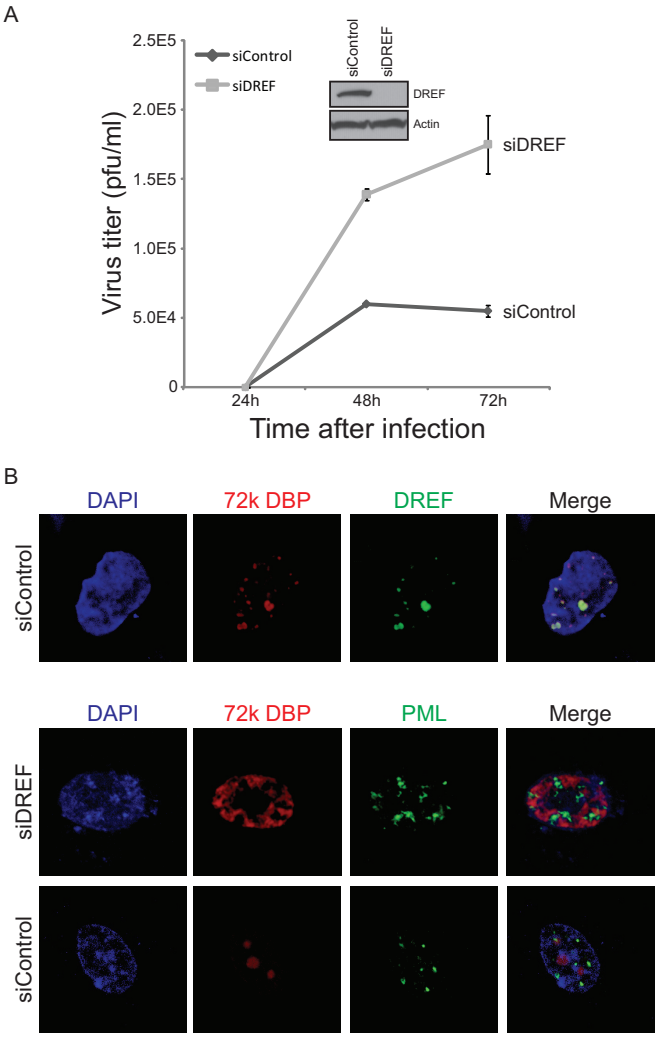

FIG 6 DREF restricts HAdV growth and colocalizes with viral replication centers. (A) DREF was knocked down in HT1080 cells using DREF-specific siRNA (siDREF); nonspecific siRNA was used as a negative control (siControl). Twenty-four hours after siRNA transfection, cells were infected with HAdV5 (*dl*309) at an MOI of 1, and viral titers were determined on 293 cells at the indicated time points ($n = 4$; error bars represent standard deviations of results for the biological replicates). (B) HT1080 cells were transfected with a plasmid expressing HA-tagged DREF, infected with HAdV5 (*dl*309) 24 h later, and imaged a further 24 h later. DREF was visualized using anti-HA (3F10) antibody, and 72k DBP was detected using monoclonal anti-72k DBP antibody. PML was visualized using polyclonal anti-PML antibody. The top row represents cells treated only with control siRNA and stained for 72k DBP and DREF; the middle and bottom rows represents cells that were stained for 72k DBP and PML and were treated with either DREF siRNA or control siRNA.

which functions largely by binding to cellular proteins and altering their function. The limited knowledge of the role of CR4 in the function of E1A confines our understanding of the function of this critical viral regulator and oncoprotein.

To overcome this shortcoming and better understand how this region contributes to the overall function of E1A, we undertook MS-based identification of E1A C terminus binding partners, and here we report, for the first time, the identification of DREF as a novel direct binding partner of E1A. Mapping the interaction site identified two amino acids within CR4 of E1A (L272 and L273) as important for this interaction. Other residues also seem to contribute to the interaction, such as K253 and R258; when these two residues were mutated in E1A, the mutant E1A showed reduced binding to DREF versus wild-type E1A. The interaction between E1A and DREF appears to be direct, as bacterially expressed E1A was able to pull down bacterially expressed DREF (Fig. 3) and examination of the binding properties of the E1A mutants used in this study toward other proteins that bind in the same regions reveals very different patterns (Table 1). Importantly, loss of binding to some factors by E1A or reduced binding to them enhances binding to DREF, suggesting overlapping but not exclusive regions of interaction (for example, the E1A R258E mutant that binds better to DREF than wild-type E1A largely loses binding to DYRK1A and HAN11). These observations also exclude the possibility that DREF mediates the interaction between E1A and DYRK1A or HAN11. Interestingly, we were able to observe a higher-molecular-weight isoform of DREF interacting with E1A. The apparent molecular weight of this modified DREF corresponds to SUMOylated DREF (compare Fig. 2D and 4B), suggesting that E1A retains binding to posttranslationally modified DREF.

The region of E1A surrounding residues L272/273 could potentially be a novel MoRF that is also present in cellular polypeptides (Fig. 4A) that alter SUMOylation of proteins. DREF was found to bind to all E1A proteins from all HAdV subgroups, and we show that DREF plays a role in viral gene expression and growth. Interestingly, DREF appears to have a dual function. On one hand it contributes to activation of viral gene expression early in infection. On the other hand, it restricts viral growth, as knockdown of the protein enhanced viral DNA replication and ultimately viral titers. DREF also localizes to viral replication centers, suggesting it may play a direct regulatory role in viral reproduction. We have also observed enhanced SUMOylation of DREF that was dependent on the ability of E1A to bind to DREF and UBC9. This is, as far as we are aware, the first report of E1A enhancing the SUMOylation state of a cellular protein and only the second report of E1A altering protein SUMOylation. Previously, E1A was shown to block SUMOylation of pRb (38), suggesting the importance of subjugating this cellular posttranslational machinery during viral infection. There was some variability in the ability of E1A to enhance DREF SUMOylation; this could be partly caused by the various levels of E1A expression. For example, enhancement of SUMOylation of DREF by E1A243R was the highest in Fig. 4C, and this was the isoform of E1A that was expressed at the highest levels. Nevertheless, it is clear that E1A enhances DREF SUMOylation, suggesting that it may function as a viral SUMO ligase.

DREF binds to E1A via two regions (CR3 and CR4) that appear to function independently, and each is sufficient for the interaction (Fig. 2B). The ability to bind proteins via multiple regions is a property of E1A that has been previously noted for multiple targets (2, 39–41). Although we are unsure of the consequences of DREF binding to E1A via CR3, the CR4-mediated interaction is required for the ability of E1A to enhance DREF SUMOylation (Fig. 4). Importantly, the ability to enhance DREF SUMOylation appears to require the interaction of E1A with DREF itself and UBC9, the sole cellular SUMO conjugase (42). The identification of a new MoRF within E1A that was also found in a cellular SUMO-specific isopeptidase, USPL1 (43), suggested that the enhancement of SUMOylation observed may be a passive process through inhibition of possible interaction between DREF and USPL1. However, UBC9 is also required for enhanced DREF

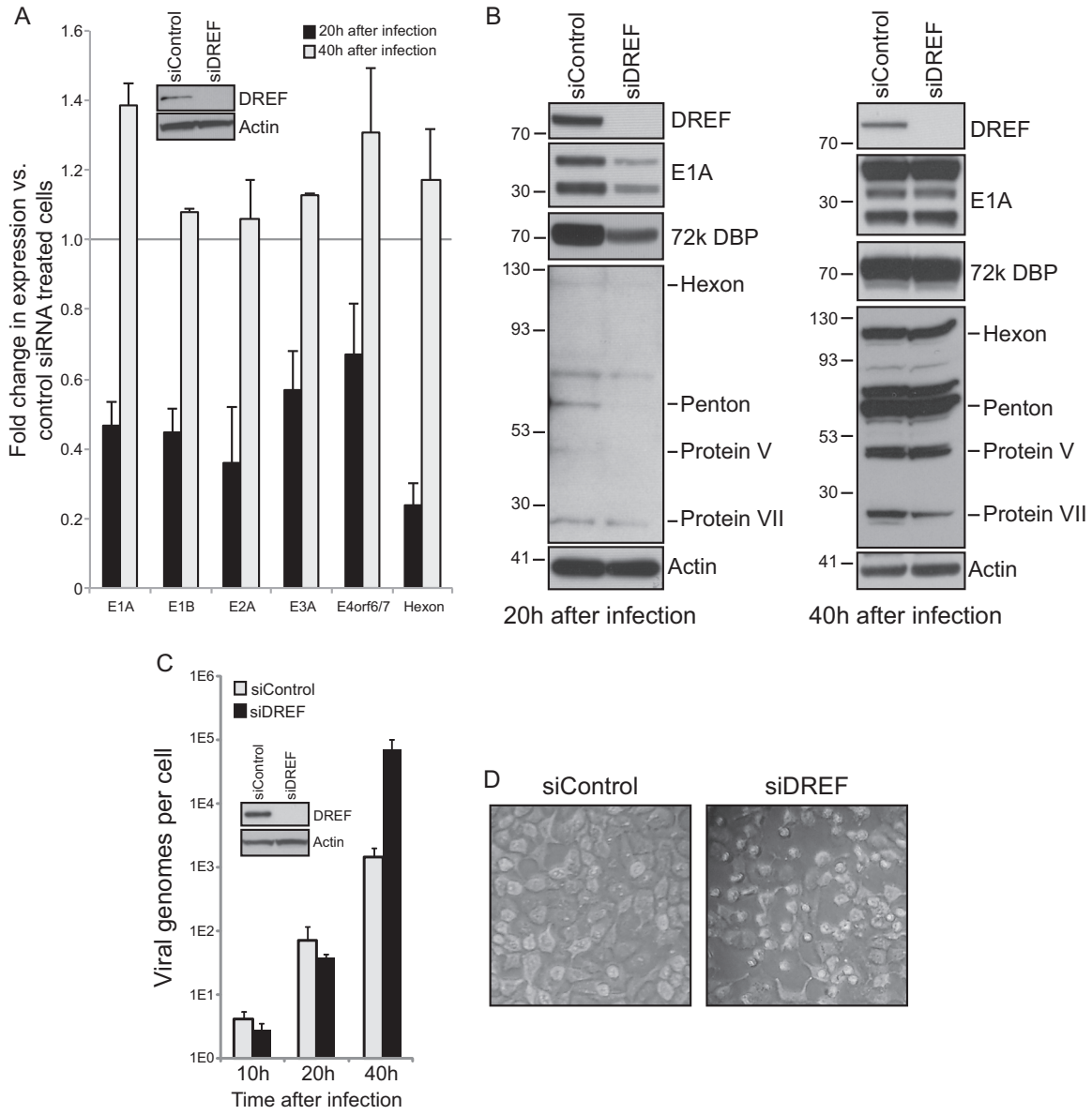

FIG 7 DREF coregulates viral gene expression and suppresses viral genome replication. (A) HT1080 cells were treated with siRNA for DREF or a negative-control siRNA. Twenty-four hours after siRNA transfection cells were infected with HAdV5 (*dl*309) at an MOI of 10, and total RNA was extracted 20 and 40 h after infection using TRIzol reagent. mRNA levels were quantified using real-time quantitative PCR and normalized to GAPDH (glyceraldehyde-3-phosphate dehydrogenase). The levels were plotted as fold changes versus the level for control siRNA-treated cells, set to 1 ($n = 7$; error bars represent standard deviations of the results for biological replicates). (B) Representative Western blots of E1A, 72k DBP, and viral structural proteins at 20 and 40 h after HAdV5 infection with *dl*309 at an MOI of 10 in DREF knockdown and control knockdown cells. E1A was detected using M73 anti-E1A monoclonal antibody, 72k DBP was detected using anti-DBP monoclonal antibody, and viral structural proteins were detected using polyclonal anti-adenovirus 5 antibody. Twenty micrograms of total cell lysate was loaded per lane, and samples were resolved on a 4 to 12% gradient Novex Bolt gel. (C) HT1080 cells were treated with siRNA for DREF or a negative-control siRNA. Twenty-four hours after siRNA transfection cells were infected with HAdV5 (*dl*309) at an MOI of 10, and low-molecular-weight DNA was extracted at the indicated time points after infection as described in Materials and Methods. Viral genomes were quantified using qPCR with primers recognizing the E1B region, with the pXC1 plasmid used to generate the standard curve. The data are plotted as genome copies per cell, and error bars represent standard deviations of results for biological replicates ($n = 4$). (D) Same cells as in panel C prior to harvest for viral DNA content analysis imaged at 40 h after HAdV5 (*dl*309) infection showing cellular morphology. Magnification, ×100.

SUMOylation (Fig. 4C), which suggests that this process is more active. One possible mechanism may involve corecruitment of UBC9 and DREF via simultaneous binding to E1A and at the same time competitive inhibition of binding by USPL1. Together, these would ensure maximal DREF SUMOylation. It is tempting to speculate that the MoRF identified is a feature of cellular isopeptidases that recognize specific SUMOylated residues or proteins; however, E1A appears to interact with DREF regardless of its SUMOylation state, and the vast majority of DREF proteins are not SUMOylated (not shown). Interestingly, although the putative MoRF that we have identified spans much more than the two leucine residues that are required for the interaction between E1A

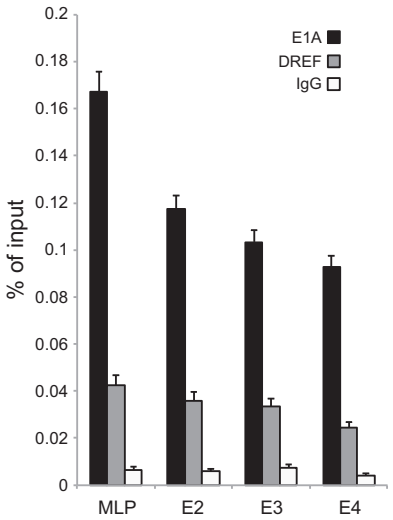

FIG 8 DREF is recruited to viral promoters. HT1080 cells were infected with HAdV5 (*dl*309) at an MOI of 10, and ChIPs were carried out 16 h after viral infection. E1A was immunoprecipitated using a cocktail of anti-E1A antibodies (M73 and M58), and DREF was immunoprecipitated using anti-DREF polyclonal antibody. 12CA5 anti-HA monoclonal antibody was used as a negative IgG control. Data are plotted as % of input sample ($n = 4$; error bars represent standard deviations of results for biological replicates).

and DREF, most other residues tested had limited impact on the interaction (Fig. 2). It is possible that the hydrophobic residues within the MoRF are necessary for the interaction, whereas the charged residues have little effect. Nevertheless, the identification of this region and its similarity to USPL1 suggested alteration in SUMOylation as a possible mechanism of E1A effects on DREF. The role of the CR3-mediated interaction with DREF is unclear, and we did not identify a sequence similar to that found in CR4 in CR3. It is possible that this interaction plays some role in E1A-mediated transcriptional regulation. An interaction between PML-II and CR3 of E1A was shown to be important for the ability of E1A to activate viral promoters (44), and since DREF is colocalized to PML bodies the two may be linked. Significantly, we observed reduced viral gene expression upon knockdown of DREF (Fig. 7).

Our observation that knockdown of DREF reduced viral gene expression early on in the infection but ultimately yielded higher viral titers suggests a dual function for DREF during the viral life cycle. Early on in the infection, DREF appears to work together with E1A as a coactivator driving viral gene expression. Previous work showed that the C-terminal portion of E1A does contribute to activation of viral gene expression (45), and this could be at least partially mediated by DREF. Although knockdown of DREF reduced both viral mRNA and protein levels (Fig. 7), these returned to normal 40 h after infection, and there was no observable difference in either viral gene expression or protein levels. This suggests that redundancy in E1A may overcome this defect at later times during infection, or it is possible that the higher viral genome numbers observed later in the infection compensated for the reduced ability of E1A to activate viral promoters in the absence of DREF. The more critical role for DREF, however, appears to be its function as a viral restriction factor, perhaps in conjunction with other PML-associated proteins. PML-associated proteins appear to play an important role in cellular intrinsic antiviral immunity (34, 46). It is likely that the antiviral functions of DREF have a greater effect on total viral titers than its role in viral gene expression, and therefore when DREF is knocked down, viral titers go up. This is further supported by viral gene expression "catching up" to normal levels even in DREF knockdown cells at later times. This is likely due to higher viral genome numbers present later on in the infection, as we have observed nearly a 100-fold increase in viral genome numbers per cell at 40 h after infection in DREF knockdown cells versus control knockdown cells, and this was also associated with earlier appearance of CPE (Fig. 7). Nevertheless, the virus appears to use this cellular protein in two very different ways in order to ensure maximum efficiency of viral reproduction.

Subcellular redistribution of endogenous proteins within infected cells appears to be a common mechanism of E1A function, as we have previously observed this with Nek9 (27). E1A appears to relocalize DREF from directly overlapping with PML to a peripheral position in PML bodies (Fig. 5). Furthermore, during the course of viral infection DREF is relocalized to viral replication centers, and it is perhaps here that its antiviral role is more important. Indeed, a recent report has shown a similar effect on another PML-associated protein, Sp100, and highlighted its role in antiviral response (34). Interestingly, we observed a change in the morphology of viral replication centers in DREF knockdown cells (Fig. 6B). The much larger distribution of viral replication centers observed suggests a viral infection that is further along than what is seen in control cells, where the replication centers are individual spots within the nucleus (Fig. 6B, bottom panel). This is further supported by earlier appearance of CPE in DREF knockdown cells as well as enhanced viral genome numbers.

In addition to playing a role in viral gene expression and growth, DREF may be important for E1A-induced cellular transformation. Mutations of the two residues required for the interaction with DREF lead to inability of E1A to transform primary rodent cells in cooperation with E1B (19), although it is unclear whether this is due to the loss of binding to DREF or DYRK1A. The *Drosophila* homologue of DREF is an important coregulator

TABLE 1 Ability of the 289R E1A C-terminal substitution mutants to bind the indicated cellular proteins

Cellular protein	Binding ability[a] of E1A							
	wt	P248A	K253E	R258E	R262/263E	E267K	D271K	L272/273A
DREF	+++	++++	++	++++	+	+++	+++	−
FOXK1	++++	++++	++++	++++	++++	++++	++++	++++
DYRK1A	+++	++	+	−	−	++	−	−
HAN11	++++	++	+	±	±	++	−	±
CtBP	+++	+++	+++	+++	+++	++	++	+++

[a] − indicates no binding, ± denotes very weak binding, and the number of + signs indicates the strength of binding.

of genes involved in control of cellular growth (47), and the human protein has also been implicated in regulation of similar cellular activities (36). Therefore, it is tempting to speculate that, in addition to regulating viral growth, interaction of E1A with DREF is important for cell cycle induction although further experimentation is needed to test this possibility.

Decades of study have identified only five binding partners of the E1A C terminus. This number is staggeringly low compared to the number for the rest of the E1A protein, which binds to a much larger repertoire of cellular proteins (6). Our identification of DREF as a novel C terminus binding factor increases our understanding of this region of E1A and expands our limited understanding of DREF function. The role of DREF in infection appears complex, as it can act as a coactivator of viral gene expression and a viral restriction factor. DREF was also identified to be SUMOylated and targeted to PML bodies in uninfected cells and to viral replication centers during HAdV infection. We have only just begun to understand the role of DREF in the cell and during the course of viral infection. Our findings reveal the complexity of virus-host interactions and will assist in future studies of how DREF affects HAdV biology and its role in uninfected cells.

ACKNOWLEDGMENTS

This work was supported by grants from the Natural Sciences and Engineering Research Council (grant number RGPIN/435375-2013) and Manitoba Medical Service Foundation (grant number MMSF 8-2013-04) to P.P. Partial funding was provided by a Canadian Institutes of Health Research operating grant to J.S.M. (grant number MOP-111173). S.R. was supported by the University of Manitoba Graduate Student Scholarship, M.K. was supported by the University of Manitoba Faculty of Science Studentship and Jack Prior Memorial Award, and R.J. was supported by an NSERC Studentship.

We are grateful to Fumiko Hirose for the HA-tagged DREF construct, Arnie Berk for pAdLoxP-WRE-SV40 and 293CRE cells, Phil Branton for the 72k DBP hybridoma supernatant, Frank Graham for Ad-LacZ and 293 cells, Ron Hay for HA-tagged SUMO constructs, and Peter Whyte for 9E10 hybridoma and pCAN-myc vector. S.R. thanks Jerzy and Mariola Radko for their guidance and support. P.P. thanks Jolen Galaugher for assistance with the manuscript. P.P. also thanks Stanislawa Pelka for invaluable support and assistance.

REFERENCES

1. **Pelka P, Ablack JN, Torchia J, Turnell AS, Grand RJ, Mymryk JS.** 2009. Transcriptional control by adenovirus E1A conserved region 3 via p300/CBP. Nucleic Acids Res. **37:**1095–1106. http://dx.doi.org/10.1093/nar/gkn1057.
2. **Pelka P, Miller MS, Cecchini M, Yousef AF, Bowdish DM, Dick F, Whyte P, Mymryk JS.** 2011. Adenovirus E1A directly targets the E2F/DP-1 complex. J. Virol. **85:**8841–8851. http://dx.doi.org/10.1128/JVI.00539-11.
3. **Whyte P, Buchkovich KJ, Horowitz JM, Friend SH, Raybuck M, Weinberg RA, Harlow E.** 1988. Association between an oncogene and an anti-oncogene: the adenovirus E1A proteins bind to the retinoblastoma gene product. Nature **334:**124–129. http://dx.doi.org/10.1038/334124a0.
4. **Shenk T, Flint J.** 1991. Transcriptional and transforming activities of the adenovirus E1A proteins. Adv. Cancer Res. **57:**47–85. http://dx.doi.org/10.1016/S0065-230X(08)60995-1.
5. **Bayley S, Mymryk J.** 1994. Adenovirus e1a proteins and transformation (review). Int. J. Oncol. **5:**425–444.
6. **Pelka P, Ablack JN, Fonseca GJ, Yousef AF, Mymryk JS.** 2008. Intrinsic structural disorder in adenovirus E1A: a viral molecular hub linking multiple diverse processes. J. Virol. **82:**7252–7263. http://dx.doi.org/10.1128/JVI.00104-08.
7. **Albert R.** 2005. Scale-free networks in cell biology. J. Cell Sci. **118:**4947–4957. http://dx.doi.org/10.1242/jcs.02714.
8. **Almaas E.** 2007. Biological impacts and context of network theory. J. Exp. Biol. **210:**1548–1558. http://dx.doi.org/10.1242/jeb.003731.
9. **Madan Babu M, Balaji S, Aravind L.** 2007. General trends in the evolution of prokaryotic transcriptional regulatory networks. Genome Dyn. **3:**66–80. http://dx.doi.org/10.1159/000107604.
10. **Xue Q, Miller-Jensen K.** 2012. Systems biology of virus-host signaling network interactions. BMB Rep. **45:**213–220. http://dx.doi.org/10.5483/BMBRep.2012.45.4.213.
11. **Rozenblatt-Rosen O, Deo RC, Padi M, Adelmant G, Calderwood MA, Rolland T, Grace M, Dricot A, Askenazi M, Tavares M, Pevzner SJ, Abderazzaq F, Byrdsong D, Carvunis AR, Chen AA, Cheng J, Correll M, Duarte M, Fan C, Feltkamp MC, Ficarro SB, Franchi R, Garg BK, Gulbahce N, Hao T, Holthaus AM, James R, Korkhin A, Litovchick L, Mar JC, Pak TR, Rabello S, Rubio R, Shen Y, Singh S, Spangle JM, Tasan M, Wanamaker S, Webber JT, Roecklein-Canfield J, Johannsen E, Barabasi AL, Beroukhim R, Kieff E, Cusick ME, Hill DE, Munger K, Marto JA, Quackenbush J, Roth FP, et al.** 2012. Interpreting cancer genomes using systematic host network perturbations by tumour virus proteins. Nature **487:**491–495. http://dx.doi.org/10.1038/nature11288.
12. **Ferrari R, Berk AJ, Kurdistani SK.** 2009. Viral manipulation of the host epigenome for oncogenic transformation. Nat. Rev. Genet. **10:**290–294. http://dx.doi.org/10.1038/nrg2539.
13. **Ferrari R, Su T, Li B, Bonora G, Oberai A, Chan Y, Sasidharan R, Berk AJ, Pellegrini M, Kurdistani SK.** 2012. Reorganization of the host epigenome by a viral oncogene. Genome Res. **22:**1212–1221. http://dx.doi.org/10.1101/gr.132308.111.
14. **Yousef AF, Fonseca GJ, Cohen MJ, Mymryk JS.** 2012. The C-terminal region of E1A: a molecular tool for cellular cartography. Biochem. Cell Biol. **90:**153–163. http://dx.doi.org/10.1139/o11-080.
15. **Boyd JM, Subramanian T, Schaeper U, La Regina M, Bayley S, Chinnadurai G.** 1993. A region in the C-terminus of adenovirus 2/5 E1a protein is required for association with a cellular phosphoprotein and important for the negative modulation of T24-ras mediated transformation, tumorigenesis and metastasis. EMBO J. **12:**469–478.
16. **Zhang Z, Smith MM, Mymryk JS.** 2001. Interaction of the E1A oncoprotein with Yak1p, a novel regulator of yeast pseudohyphal differentiation, and related mammalian kinases. Mol. Biol. Cell **12:**699–710. http://dx.doi.org/10.1091/mbc.12.3.699.
17. **Komorek J, Kuppuswamy M, Subramanian T, Vijayalingam S, Lomonosova E, Zhao LJ, Mymryk JS, Schmitt K, Chinnadurai G.** 2010. Adenovirus type 5 E1A and E6 proteins of low-risk cutaneous beta-human papillomaviruses suppress cell transformation through interaction with FOXK1/K2 transcription factors. J. Virol. **84:**2719–2731. http://dx.doi.org/10.1128/JVI.02119-09.
18. **Kohler M, Gorlich D, Hartmann E, Franke J.** 2001. Adenoviral E1A protein nuclear import is preferentially mediated by importin alpha3 in vitro. Virology **289:**186–191. http://dx.doi.org/10.1006/viro.2001.1151.
19. **Cohen MJ, Yousef AF, Massimi P, Fonseca GJ, Todorovic B, Pelka P, Turnell AS, Banks L, Mymryk JS.** 2013. Dissection of the C-terminal region of E1A re-defines the roles of CtBP and other cellular targets in oncogenic transformation. J. Virol. **87:**10348–10355. http://dx.doi.org/10.1128/JVI.00786-13.
20. **Ohshima N, Takahashi M, Hirose F.** 2003. Identification of a human homologue of the DREF transcription factor with a potential role in regulation of the histone H1 gene. J. Biol. Chem. **278:**22928–22938. http://dx.doi.org/10.1074/jbc.M303109200.
21. **Harlow E, Franza BR, Jr, Schley C.** 1985. Monoclonal antibodies specific for adenovirus early region 1A proteins: extensive heterogeneity in early region 1A products. J. Virol. **55:**533–546.
22. **Niman HL, Houghten RA, Walker LE, Reisfeld RA, Wilson IA, Hogle JM, Lerner RA.** 1983. Generation of protein-reactive antibodies by short peptides is an event of high frequency: implications for the structural basis of immune recognition. Proc. Natl. Acad. Sci. U. S. A. **80:**4949–4953. http://dx.doi.org/10.1073/pnas.80.16.4949.
23. **Evan GI, Lewis GK, Ramsay G, Bishop JM.** 1985. Isolation of monoclonal antibodies specific for human c-myc proto-oncogene product. Mol. Cell. Biol. **5:**3610–3616.
24. **Reich NC, Sarnow P, Duprey E, Levine AJ.** 1983. Monoclonal antibodies which recognize native and denatured forms of the adenovirus DNA-binding protein. Virology **128:**480–484. http://dx.doi.org/10.1016/0042-6822(83)90274-X.
25. **Hardy S, Kitamura M, Harris-Stansil T, Dai Y, Phipps ML.** 1997.

Construction of adenovirus vectors through Cre-lox recombination. J. Virol. **71:**1842–1849.
26. **Harlow E, Lane D.** 1999. Using antibodies: a laboratory manual. Cold Spring Harbor Laboratory Press, Cold Spring Harbor, NY.
27. **Pelka P, Scime A, Mandalfino C, Joch M, Abdulla P, Whyte P.** 2007. Adenovirus E1A proteins direct subcellular redistribution of Nek9, a NimA-related kinase. J. Cell. Physiol. **212:**13–25. http://dx.doi.org/10.1002/jcp.20983.
28. **Tatham MH, Jaffray E, Vaughan OA, Desterro JM, Botting CH, Naismith JH, Hay RT.** 2001. Polymeric chains of SUMO-2 and SUMO-3 are conjugated to protein substrates by SAE1/SAE2 and Ubc9. J. Biol. Chem. **276:**35368–35374. http://dx.doi.org/10.1074/jbc.M104214200.
29. **Pfaffl MW.** 2001. A new mathematical model for relative quantification in real-time RT-PCR. Nucleic Acids Res. **29:**e45. http://dx.doi.org/10.1093/nar/29.9.e45.
30. **Hutten S, Chachami G, Winter U, Melchior F, Lamond AI.** 2014. A role for the Cajal-body-associated SUMO isopeptidase USPL1 in snRNA transcription mediated by RNA polymerase II. J. Cell Sci. **127:**1065–1078. http://dx.doi.org/10.1242/jcs.141788.
31. **Yousef AF, Fonseca GJ, Pelka P, Ablack JN, Walsh C, Dick FA, Bazett-Jones DP, Shaw GS, Mymryk JS.** 2010. Identification of a molecular recognition feature in the E1A oncoprotein that binds the SUMO conjugase UBC9 and likely interferes with polySUMOylation. Oncogene **29:**4693–4704. http://dx.doi.org/10.1038/onc.2010.226.
32. **Hateboer G, Hijmans EM, Nooij JB, Schlenker S, Jentsch S, Bernards R.** 1996. mUBC9, a novel adenovirus E1A-interacting protein that complements a yeast cell cycle defect. J. Biol. Chem. **271:**25906–25911. http://dx.doi.org/10.1074/jbc.271.42.25906.
33. **Eskiw CH, Dellaire G, Mymryk JS, Bazett-Jones DP.** 2003. Size, position and dynamic behavior of PML nuclear bodies following cell stress as a paradigm for supramolecular trafficking and assembly. J. Cell Sci. **116:**4455–4466. http://dx.doi.org/10.1242/jcs.00758.
34. **Berscheminski J, Wimmer P, Brun J, Ip WH, Groitl P, Horlacher T, Jaffray E, Hay RT, Dobner T, Schreiner S.** 2014. Sp100 isoform-specific regulation of human adenovirus 5 gene expression. J. Virol. **88:**6076–6092. http://dx.doi.org/10.1128/JVI.00469-14.
35. **Ou HD, Kwiatkowski W, Deerinck TJ, Noske A, Blain KY, Land HS, Soria C, Powers CJ, May AP, Shu X, Tsien RY, Fitzpatrick JA, Long JA, Ellisman MH, Choe S, O'Shea CC.** 2012. A structural basis for the assembly and functions of a viral polymer that inactivates multiple tumor suppressors. Cell **151:**304–319. http://dx.doi.org/10.1016/j.cell.2012.08.035.
36. **Yamashita D, Sano Y, Adachi Y, Okamoto Y, Osada H, Takahashi T, Yamaguchi T, Osumi T, Hirose F.** 2007. hDREF regulates cell proliferation and expression of ribosomal protein genes. Mol. Cell. Biol. **27:**2003–2013. http://dx.doi.org/10.1128/MCB.01462-06.
37. **Matsukage A, Hirose F, Yoo MA, Yamaguchi M.** 2008. The DRE/DREF transcriptional regulatory system: a master key for cell proliferation. Biochim. Biophys. Acta **1779:**81–89. http://dx.doi.org/10.1016/j.bbagrm.2007.11.011.
38. **Ledl A, Schmidt D, Muller S.** 2005. Viral oncoproteins E1A and E7 and cellular LxCxE proteins repress SUMO modification of the retinoblastoma tumor suppressor. Oncogene **24:**3810–3818. http://dx.doi.org/10.1038/sj.onc.1208539.
39. **Bruton RK, Pelka P, Mapp KL, Fonseca GJ, Torchia J, Turnell AS, Mymryk JS, Grand RJ.** 2008. Identification of a second CtBP binding site in adenovirus type 5 E1A conserved region 3. J. Virol. **82:**8476–8486. http://dx.doi.org/10.1128/JVI.00248-08.
40. **Pelka P, Ablack JN, Shuen M, Yousef AF, Rasti M, Grand RJ, Turnell AS, Mymryk JS.** 2009. Identification of a second independent binding site for the pCAF acetyltransferase in adenovirus E1A. Virology **391:**90–98. http://dx.doi.org/10.1016/j.virol.2009.05.024.
41. **Dyson N, Guida P, McCall C, Harlow E.** 1992. Adenovirus E1A makes two distinct contacts with the retinoblastoma protein. J. Virol. **66:**4606–4611.
42. **Jentsch S, Psakhye I.** 2013. Control of nuclear activities by substrate-selective and protein-group SUMOylation. Annu. Rev. Genet. **47:**167–186. http://dx.doi.org/10.1146/annurev-genet-111212-133453.
43. **Schulz S, Chachami G, Kozaczkiewicz L, Winter U, Stankovic-Valentin N, Haas P, Hofmann K, Urlaub H, Ovaa H, Wittbrodt J, Meulmeester E, Melchior F.** 2012. Ubiquitin-specific protease-like 1 (USPL1) is a SUMO isopeptidase with essential, non-catalytic functions. EMBO Rep. **13:**930–938. http://dx.doi.org/10.1038/embor.2012.125.
44. **Berscheminski J, Groitl P, Dobner T, Wimmer P, Schreiner S.** 2013. The adenoviral oncogene E1A-13S interacts with a specific isoform of the tumor suppressor PML to enhance viral transcription. J. Virol. **87:**965–977. http://dx.doi.org/10.1128/JVI.02023-12.
45. **Mymryk JS, Bayley ST.** 1993. Induction of gene expression by exon 2 of the major E1A proteins of adenovirus type 5. J. Virol. **67:**6922–6928.
46. **Schreiner S, Wodrich H.** 2013. Virion factors that target Daxx to overcome intrinsic immunity. J. Virol. **87:**10412–10422. http://dx.doi.org/10.1128/JVI.00425-13.
47. **Kawamori A, Shimaji K, Yamaguchi M.** 2013. Control of e2f1 and PCNA by Drosophila transcription factor DREF. Genesis **51:**741–750. http://dx.doi.org/10.1002/dvg.22419.